

Brain Stimulation Improves Cognitive Control by Modulating Medial-Frontal Activity and preSMA-vmPFC Functional Connectivity

Jiaxin Yu,^{1,2} Philip Tseng,^{3,4} Daisy L. Hung,² Shih-Wei Wu,¹ and Chi-Hung Juan^{2*}

¹*Institute of Neuroscience, National Yang-Ming University, Taipei City, Taiwan*

²*Institute of Cognitive Neuroscience, National Central University, Taiwan*

³*Graduate Institute of Humanities in Medicine, Taipei Medical University, Taipei, Taiwan*

⁴*Brain and Consciousness Research Center, Shuang-Ho Hospital, New Taipei City, Taiwan*

Abstract: Previous research has demonstrated that brain stimulation can improve inhibitory control. However, the neural mechanisms underlying such artificially induced improvement remain unclear. In this study, by coupling anodal transcranial direct current stimulation (atDCS) with functional MRI, we found that atDCS over preSMA effectively improved stopping speed, which was associated with increased BOLD response in the preSMA and ventromedial prefrontal cortex (vmPFC). Furthermore, such atDCS-induced BOLD increase in vmPFC was positively correlated with participants' improvement in stopping efficiency, and the functional connectivity between preSMA and vmPFC increased during successful stop. These results suggest that the rapid behavioral improvement from preSMA brain stimulation involves modulated medial-frontal activity and preSMA-vmPFC functional connectivity. *Hum Brain Mapp* 36:4004–4015, 2015. © 2015 Wiley Periodicals, Inc.

Key words: response inhibition; tDCS; fMRI; preSMA; vmPFC

INTRODUCTION

Cognitive control reflects the ability to suppress a prepotent response and is an important cognitive ability in almost every aspect of our daily life. This ability has been identified as a reliable predictor of school performance and

socioeconomic status even 30 years later (Moffitt et al., 2011), whereas a decline in this ability is commonly found in many forms of mental illness such as depression and substance abuse [Diamond, 2013]. Neuroimaging studies have implicated a network of regions that together form the “stopping network” that supports the processes involved in inhibitory control. This network includes the presupplementary motor area (preSMA), right inferior frontal gyrus (rIFG), subthalamic nucleus, dorsolateral prefrontal cortex (DLPFC), medial prefrontal cortex (mPFC), and posterior parietal cortex (PPC) [Aron and Poldrack, 2006; Li et al., 2006; Zandbelt et al., 2013]. Further evidence from granger causality analysis [Duann et al., 2009] and transcranial magnetic stimulation studies (TMS) [Rushworth et al., 2002; Taylor et al., 2007; Chen et al., 2009; Juan and Muggleton, 2012] suggest that preSMA may play a causal role, along with other regions, in mediating inhibitory control.

Recently, considerable progress has been made in improving people's cognitive ability, such as visual

Contract grant sponsor: Ministry of Science and Technology, Taiwan; Contract grant numbers: 103-2410-H-008 -023 -MY3, 101-2628-H-008-001-MY4, 102-2420-H-008-001-MY3, 101-2410-H-008-033-MY3.

*Correspondence to: Chi-Hung Juan, PhD, Institute of Cognitive Neuroscience, National Central University No. 300, Jhongda Rd. Jhongli City, 320, Taiwan. E-mail: chijuan@cc.ncu.edu.tw

Received for publication 29 April 2015; Revised 13 June 2015; Accepted 27 June 2015.

DOI: 10.1002/hbm.22893

Published online 7 August 2015 in Wiley Online Library (wileyonlinelibrary.com).

short-term memory [Tseng et al., 2012] and response inhibition [Hsu et al., 2011; Jacobson et al., 2011], via the use of noninvasive electrical stimulation. With 10 min of anodal transcranial direct current stimulation (atDCS) over preSMA, participants showed significant improvement in their inhibitory control [Hsu et al., 2011]. These findings of cognitive enhancement, however, have generated much debate over whether tDCS really works beyond the motor cortex, and if it does, does it work in every individual [for reviews and opinions from both sides, see Antals et al., 2015; Horvath et al., 2015a,b]. Indeed, although researchers have proposed many considerations such as baseline neuronal activity [Li et al., 2015], individual cognitive ability [Tseng et al., 2012], or task difficulty [Wu et al., 2014] to address the issue of replicability in tDCS studies, at the heart of this debate is the lack of neuroimaging data to push forward our understanding of the mechanisms behind tDCS. In addition, since electric current tends to travel within the brain via paths of least resistance, without any neuroimaging evidence, it is also not possible to know whether atDCS improved inhibitory control via a simple modulation of only the stimulated area or in a network-like fashion. Thus, it is reasonable to suspect an atDCS effect in areas that are functionally or anatomically connected to preSMA. In our opinion, improving the knowledge of the neural mechanisms whereby external stimulation improves cognitive control is vital, both from a basic research and a clinical perspective. Furthermore, the combination of neuroimaging and causal techniques can offer converging and insightful understandings of the inhibitory control system. To this end, in this study we used fMRI to investigate the neural basis of tDCS-mediated improvement in inhibitory control.

Two experiments were run in this study, one tDCS-behavior only (Experiment 1) and one with tDCS and fMRI (Experiment 2). Experiment 1 was done to assess the effect of practice (sham day) versus tDCS (active tDCS day). To anticipate our results, since we observed no practice effect (presham vs. postsham performance) or order effect (sham day first vs. active tDCS day first) from Experiment 1, we simplified the design of Experiment 2 to a sham-then-tDCS design so that all participants could finish the sham and active tDCS sessions in one day.

MATERIALS AND METHODS

Subjects

Eight participants (age range: 20–31 years, 5 males, and 3 females) took part in experiment 1 and 23 participants (age range: 20–28 years, 13 males, and 10 females) took part in experiment 2. All participants gave informed consent prior to the start of the experimental session. All reported being free of neurological or psychological medical problems and all had normal or corrected-to-normal vision. The experimental procedures here were approved

by the Institutional Review Board of the Chang Gung Memorial Hospital, Linkou, Taiwan.

Stop Signal Task

In the laboratory, cognitive control is often investigated using a stop-signal paradigm [Logan et al., 1984], where a “go” signal requires a motor response from the participants, but an irregularly intervening sudden “stop” signal requires the response to be inhibited. Participants were required to press the left or right button of response box with their left or right index finger according to the direction of a “go” arrow. In 70% of the trials, this made up the entire trial (go trials). In the remaining 30% of trials, a red dot (stop signal) appeared shortly after the go signal, prompting the participants to withhold their go response. The stop signal task consisted of 140 go trials and 60 stop trials in one block, and there were three blocks in each condition (four conditions in experiment 1: prestimulation vs. poststimulation and sham vs. atDCS; two conditions in experiment 2: sham and atDCS). Participants had to respond to the corresponding arrow direction by default, but to withhold their actions when a stop signal was presented at the center of the screen after the left/right arrow. The stimulus onset asynchrony between go signal and stop signal is called the stop signal delay (SSD), and it was dynamically adjusted in a staircase fashion for each individual so that all participants performed around 50% correct in trials with a stop signal. This adaptation tracking method can eliminate practice effect, since the difficulty level was around 50%. The intertrial interval was randomly varied from an exponential distribution with a mean of 1 s and range between 0.5 and 4 s.

Procedures

Experiment 1

All participants received sham and anodal conditions on two separated days within one week in a within-group counterbalanced sequence. In the practice session, participants first received 80 “go” trials to set a response time threshold for each individual’s critical go RT (by using the mean + 2 × std of the 80 go trials), and had additional 70 go trials and 30 stop trials that provided auditory feedback if their reaction times were longer than their critical go RT. The individual mean SSD from the practice session would be set as their initial SSD for the formal experiment. In the formal experiment, participants first performed the prestimulation session, then received sham or anodal stimulation, and performed the poststimulation session. The purposes of Experiment 1 are to examine whether atDCS over FZ would enhance response inhibition and to differentiate the practice effect, if any, from the atDCS effect (if any) in response inhibition.

Experiment 2

The training and testing phases were distributed across two days. All participants received a training session that

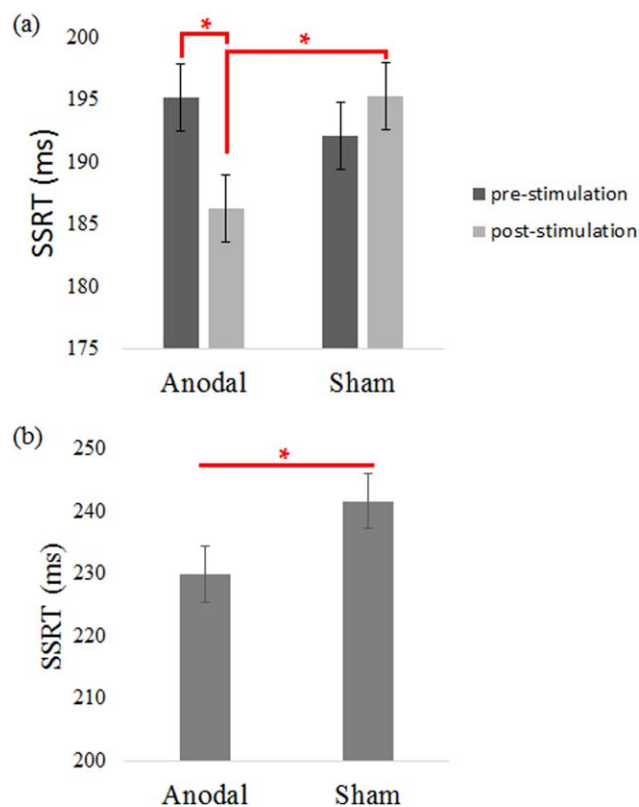


Figure 1.

(a) Experiment 1 shows that the behavioral improvement is mainly an effect of atDCS. In the sham condition, there is no evidence of practice or order effect in behavioral performances. (b) Experiment 2 replicates this atDCS facilitation in the fMRI sessions. [Color figure can be viewed in the online issue, which is available at wileyonlinelibrary.com.]

was identical to the formal fMRI experiment to make sure they perfectly understood the task requirements, and to minimize possible practice effects by stabilizing their performance level through training. All trial design and task details were identical as Experiment 1 except the simplified sham-then-active-tDCS procedure here: participants first performed the Sham condition in the scanner, then received atDCS outside the scanner, and went back into the scanner to perform stop signal task again.

Behavioral Analysis

The mean and variation of go RTs were estimated after removing incorrect response trials. Trials were also excluded, which had latencies longer and shorter than 2.5 times the standard deviations away from each subject's mean go RT for each condition. The primary measure of interest, stop signal reaction time (SSRT), reflects individual stop latency and is used as an index subject's inhibitory control, a shorter SSRT indicates a better inhibitory control in individuals. SSRT is estimated by subtracting mean SSD from mean reaction time of go trials [Band et al., 2003]. Posterror slowing, an index of strategy adjustment by examining how much response times increase following an error, was also analyzed to evaluate the effects of atDCS. If the atDCS is affecting participants' strategy adjustment, we should observe increased posterror slowing RT in both the neutral condition in the main experiment and the control experiment. For calculating post-error slowing, successful go trials were categorized into two types: go trials after a correct go trial (pG) and go trials after a stop-respond trial (pSR; unsuccessful stop).

tDCS Procedure

tDCS was delivered with an Eldith DC-stimulator via one 4 × 4 cm stimulation electrode and one 5 × 7 cm reference electrode, both housed in saline-soaked sponge coverings [Nitsche et al., 2007]. The center of the stimulation electrode (anodal) was placed over the preSMA (with the center of the electrode placed on the FZ site, 10-20 EEG system) and the reference electrode (cathodal) was placed over the left cheek. In the active atDCS condition, the current was applied for 20 min (with additional 15 s fade-in and fade-out each) with strength of 2 mA. The parameters of sham tDCS were identical to those of the active condition, except that the current was only applied for 30 s.

MRI Data Acquisition

All images were acquired with a Siemens Skyra 3-T scanner in the Taiwan Mind and Brain Imaging Center at National Chengchi University, Taipei, Taiwan. A T1 weighted magnetization-prepared rapid-acquisition gradient echo (MPRAGE) image was acquired for each subject for registration purposes (TR = 2530 ms; TE = 3.03 ms; FOV = 256 × 256 mm²; matrix = 192 × 192; slice

TABLE I. Behavioral performances from experiment 1 (mean ± standard error)

Variables	Pre-Sham	Post-Sham	Pre-atDCS	Post-atDCS
Go accuracy (%)	97.6 ± 0.8	97.1 ± 1.2	98.8 ± 0.4	98.8 ± 0.4
Mean Go RT (ms)	366.8 ± 14.8	370.6 ± 14.8	372.1 ± 10.7	389.6 ± 16.0
SSRT (ms)	192.0 ± 3.4	195.1 ± 2.1	195.2 ± 4.8	186.2 ± 3.8 (*)
SR rate (%)	48.3 ± 1.0	48.7 ± 0.9	49.7 ± 0.4	49.7 ± 0.8
SR RT (ms)	369.5 ± 12.6	371.0 ± 11.7	373.9 ± 8.8	394.5 ± 12.9

TABLE II. Behavioral performances from experiment 2 (mean ± standard error)

Variables	Sham	Anodal
Go accuracy (%)	96.4 ± 0.7	96.8 ± 0.7
Mean Go RT (ms)	457.5 ± 7.7	455.9 ± 8.2
SSRT (ms)	241.7 ± 4.5	229.9 ± 3.7 (*)
SR rate (%)	50.6 ± 0.2	50.7 ± 0.2
SR RT (ms)	448.2 ± 6.6	450.0 ± 7.4
Post-Go RT (ms)	437.0 ± 7.7	435.9 ± 10.8
Post-SR RT (ms)	442.0 ± 9.5	434.9 ± 9.0
Post-SI RT (ms)	432.2 ± 11.1	426.8 ± 10.8

thickness = 1 mm with no gap; 192 slices). Blood oxygen level dependent (BOLD) signals were then acquired with a single shot gradient echo planar imaging (EPI) sequence (TR = 2000 ms; TE = 25 ms; FOV = 220 × 220 mm²; matrix = 64 × 64; slice thickness = 3.4 mm with no gap; 37 slices) and 246 volumes were acquired in one session.

Image Preprocessing and Statistical Analysis

Image preprocessing and statistical analysis were carried out using the FMRI Expert Analysis Tool (version 6.0; part of the FSL package; FMRIB software, version 5.0.7). The first three volumes before the task were automatically discarded by the scanner to allow for T1 equilibrium. The remaining images were then realigned to correct for head motion [Jenkinson et al., 2002]. Translational movement parameters never exceeded one voxel in any direction for any subject or session. Data were spatially smoothed by using a 5-mm FWHM Gaussian kernel, and filtered in the temporal domain by using a nonlinear high-pass filter with a 100-s cutoff. All images were denoised using MELODIC [Beckmann and Smith, 2004]. Registration was performed using a two-step procedure: EPI from each scan were first registered to the MPRAGE structural image in which non-brain structures were removed using BET (Brain Extract Tool) and were then registered to the standard MNI space using 12-parameter affine transformations [Jenkinson et al., 2002]. Registration from MPRAGE structural image to standard space was further refined by using FNIRT nonlinear registration.

A standard general linear model (GLM) analyses was conducted for all data from participants. First, lower-level FEAT analysis was performed for each scan/block of each participant. Then a fixed-effect analysis was performed for each participant that combined the lower-level FEAT results from different scans using the summary statistics approach. The following events were modeled at stimulus (arrow) onset times and convolved with a double- γ hemodynamic response function: Go, Stop-Inhibit (SI), and Stop-Respond (SR). An additional nuisance regressor included incorrect and discarded Go trials. Null events were not modeled and were used as an implicit baseline. Temporal derivatives were included as covariates of no interest to improve statistical sensitivity. The SI-Go

contrast and the Stop (SI + SR) contrast were the primary contrasts of interest in this study. The output from the participant-specific analyses was then analyzed using a mixed-effects model with FLAME [Woolrich, 2008]. Group-level statistics images were thresholded with a cluster-forming threshold of $Z > 2.3$ and a cluster probability of $P < 0.05$, corrected for whole-brain multiple comparisons using Gaussian random field theory.

To explore the atDCS effects in the regions identified by the whole brain analysis, regions of interest were created independently for each subject. The leave-one-subject-out method [Esterman et al., 2010] was used in which 23 GLM were run with one subject left out in each and with each GLM defining the cluster for the subject that was left out. By drawing a 6-mm sphere around the local maxima of the activation, the ROI masks were then used to extract the parameter estimates (β) of each event type for each subject and session. Percent signal changes were calculated by multiplying [β /mean] by ppheight by 100%, where ppheight is the peak height of the hemodynamic response versus the baseline level of activity (which is determined by the event length and the convolved HRF) and the mean is the average BOLD of that ROI over time.

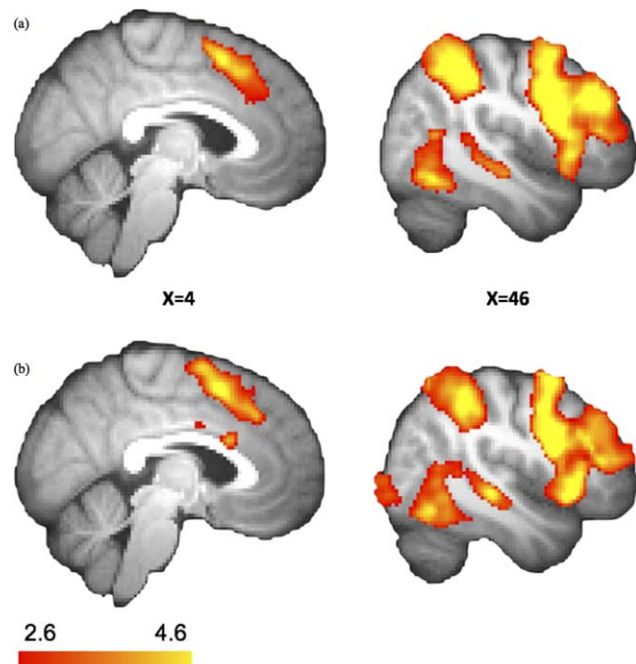


Figure 2.

The stopping network: SI > Go. Details are summarized in Table II. (a) In the sham condition, increased BOLD responses were observed in the frontal and parietal brain areas during stopping. (b) After atDCS over preSMA, the similar pattern of regional activations indicates that no additional areas were involved after atDCS. Results were corrected for multiple comparisons using cluster-based thresholding ($z = 2.6$, $P < 0.05$). [Color figure can be viewed in the online issue, which is available at wileyonlinelibrary.com.]

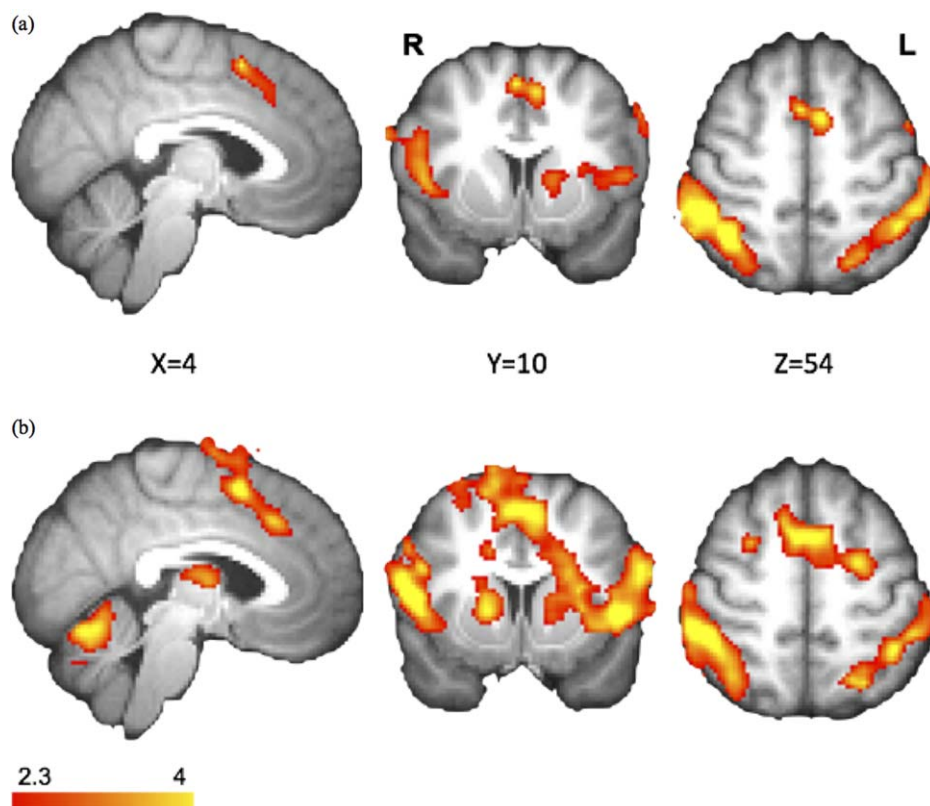


Figure 3.

Similar stopping networks in the Stop > rest contrast. Details are summarized in Table III. (a) In the sham condition, the regional activations were similar to the SI > Go contrast. (b) Increased BOLD response within the stimulation site (FZ, espe-

cially preSMA). Results were corrected for multiple comparisons using cluster-based thresholding ($z = 2.3$, $P < 0.05$). [Color figure can be viewed in the online issue, which is available at wileyonlinelibrary.com.]

To examine whether atDCS was affecting other brain regions beyond the stimulation area (i.e., preSMA), psychophysiological interaction (PPI) analysis [Cisler et al., 2014; Friston et al., 1997] was used to test for event-specific (SI) changes in areas that might be functionally connected to the stimulation area. In this analysis, preSMA was selected as a main seed ROI (MNI coordinates: 8, 8, 56; Table III). If the task-specific functional connectivity between preSMA and other regions (the stopping network or any region affected by atDCS identified by the GLM mentioned above) was enhanced by atDCS during successful stops (SI), such stop-specific connectivity can provide new information about the underlying neural mechanisms behind the observed behavioral improvements.

RESULTS

Experiment 1

atDCS selectively enhanced SSRT. No main effect was observed in the session ($F_1 = 4.057$, $P = 0.084$) and tDCS condition ($F_1 = 1.583$, $P = 0.249$), and a statistical signifi-

cance was observed in the interaction ($F_1 = 26.534$, $P < 0.001$; Fig. 1a; Table I). Posthoc comparisons showed significant differences in pre-atDCS and post-atDCS ($t_7 = 4.728$, $P = 0.002$) and in postsham and post-atDCS ($t_7 = 4.287$, $P = 0.004$). No difference of the SSRT was found in the presham and postsham condition ($t_7 = -1.657$, $P = 0.141$), presham and pre-atDCS ($t_7 = -1.078$, $P = 0.317$). These results indicate an absence of the practice effect in SSRT as Cohen and Poldrack [2008] have reported before, and therefore the effect of atDCS should not be mixed with practice or familiarization of the task. This pattern of results also allowed us to simplify the design of Experiment 2 to better suit the demand of an fMRI experiment.

Experiment 2

Behavioral results: atDCS over preSMA facilitated response inhibition

SSRT was significantly decreased after anodal stimulation ($t_{22} = 5.495$, $P < 0.001$; Fig. 1b; Table II). However, the mean Go reaction time (RT; $t_{22} = 0.291$, $P = 0.774$), Go

TABLE III. Local maxima of brain activation for the SI-Go contrast

Brain Region	Max Z	x	Y	z
Sham (cluster-level corrected $P < 0.05$, $Z > 2.3$)				
R. Middle Frontal Gyrus/Inferior Frontal Gyrus	5.96	50	12	38
R. Superior Parietal Lobule	6.94	36	-54	46
L. Superior Parietal Lobule	6.31	-30	-54	44
L. Occipital Fusiform Gyrus	6.06	-40	-64	-18
L. Precentral Gyrus	5.44	-38	2	32
R. Occipital Fusiform Gyrus	5.9	40	-66	-12
L. Insula	5.51	-30	26	0
R. Superior Frontal Gyrus/Paracingulate Gyrus	4.73	4	12	54
R. Middle Temporal Gyrus	4.9	52	-18	-12
Anodal (cluster-level corrected $P < 0.05$, $Z > 2.3$)				
R. Precentral Gyrus/Inferior Frontal Gyrus	6.5	48	8	24
R. Supramarginal Gyrus	5.94	64	-44	22
L. Temporal Occipital Fusiform Cortex	6.03	-38	-62	-18
L. Superior Parietal Lobule	5.8	-26	-58	44
R. Temporal Occipital Fusiform Cortex	6.01	34	-52	-16
L. Insula	5.43	-28	22	6
L. Precentral Gyrus	4.54	-52	6	20
L. Parietal Operculum Cortex	4.81	-60	-40	24
L. Frontal Pole	4.64	-34	38	30
R. Middle Temporal Gyrus-34	4.89	48	-28	-4
Anodal > Sham (uncorrected $P < 0.001$, $Z > 2.3$)				
R. Superior Frontal Gyrus	3.49	20	2	68

TABLE IV. Local maxima of brain activation for the stop contrasts

Brain Region	Max Z	x	y	z
Sham (cluster-level corrected $P < 0.05$, $Z > 2.3$)				
R. Lateral Occipital Cortex	6.05	26	-102	-4
L. Lateral Occipital Cortex	6.1	-44	-76	-6
R. Superior Parietal Lobule	5.58	40	-54	56
L. Postcentral Gyrus	5.13	-66	-18	26
R. Frontal Pole	4.84	28	58	24
R. Insula/Inferior Frontal Gyrus	4.82	38	18	0
L. SMA/preSMA	4.18	-6	6	52
L. Insula	4.57	-30	18	10
Anodal (cluster-level corrected $P < 0.05$, $Z > 2.3$)				
L. Lateral Occipital Cortex	6.84	-32	-92	-4
R. Cerebellum/Lateral Occipital Corte	6.39	36	-54	-32
R. Superior Frontal Gyrus/Paracingulate	5.55	12	2	72
R. Superior Parietal Lobule	5.17	32	-44	38
R. Frontal Pole	5.36	28	54	20
R. Inferior Frontal Gyrus	5.17	58	10	14
L. Superior Parietal Lobule	4.27	-42	-48	52
L. Postcentral Gyrus	4.55	-62	-20	32
R. Putamen	4.01	18	10	4
R. Postcentral Gyrus	4.61	64	-14	26
Anodal > Sham (cluster-level corrected $P < 0.05$, $Z > 2.3$)				
L. Superior Frontal Gyrus	3.71	-26	0	66
R. Frontal Medial Cortex	3.47	14	48	-8
L. Frontal Medial Cortex	3.8	-8	52	-8
R. Supplementary Motor Cortex/preSMA	3.09	8	8	56

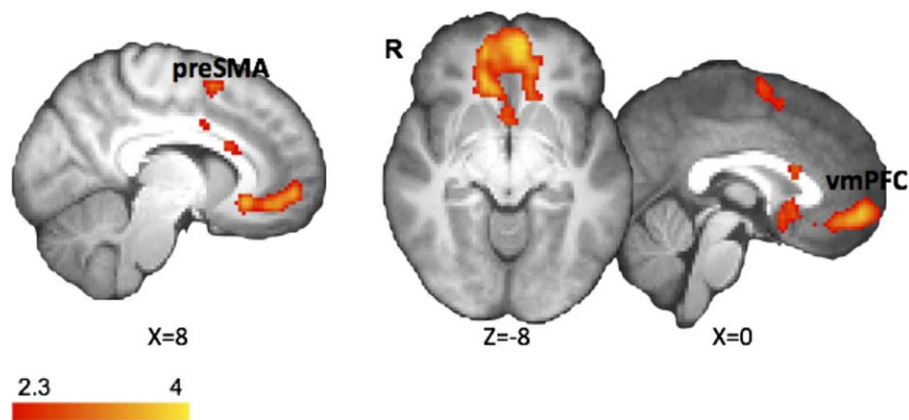


Figure 4.

Increased preSMA and vmPFC BOLD responses after atDCS. To explore the effect of atDCS in the brain, we compared different contrasts of right preSMA and vmPFC in the $Anodal_{stop} > Sham_{stop}$. Results were corrected for multiple comparisons using cluster-based thresholding ($z = 2.3$, $P < 0.05$). [Color figure can be viewed in the online issue, which is available at wileyonlinelibrary.com.]

accuracy rate ($t_{22} = -1.007$, $P = 0.325$), Stop-Respond RT ($t_{22} = -0.355$, $P = 0.726$), and Stop-Respond rate ($t_{22} = -0.522$, $P = 0.607$), PSR-PG ($t_{22} = 0.743$, $P = 0.465$) were all unaffected. These results showed that anodal stimulation over preSMA only affected stopping speed. Hence, given the fixed difficulty level (50% correct) and no effect of atDCS was observed in Go RT, SR RT, and pSR-pG, which suggests that the SSRT effect observed here was likely an atDCS effect instead of participant strategy or practice effect. If there was practice effect, we would expect to observe faster Go RT and smaller value of pSR-pG.

Regional brain activation in the sham condition

Results of the SI-Go contrast replicated regions that have been reported in previous fMRI studies: preSMA, rIFG, bilateral DLPFC, and bilateral PPC (Fig. 2a; Table III). For the Stop contrast, SMA/preSMA, right IFG, bilateral insula and superior parietal cortex were also identified (Fig. 3a; Table IV). Note that these two contrasts showed similar activation patterns.

The atDCS effects on response inhibition

After atDCS over preSMA, regions that were originally involved in response inhibition remained active in the SI-Go (Fig. 2b; Table III) and Stop contrasts (Fig. 3b; Table IV). In the SI-Go contrast, right superior frontal gyrus (rSFG) showed higher BOLD response (MNI coordinate of 20, 2, 68; $Z = 3.49$, uncorrected $P < 0.001$; Table III) after anodal stimulation compared to sham. For the Stop contrast, higher activations were observed in preSMA and ventromedial prefrontal cortex (vmPFC) in atDCS condition over sham

(corrected for multiple comparisons using cluster-based thresholding, $Z = 2.3$, $P < 0.05$; Fig. 4; Table IV).

Impact of atDCS on activity in a priori ROIs

Three ROI masks were defined based on the results from the Stop contrasts (Fig. 5a). Independent ROI analysis was conducted for the SI-Go using the above ROI masks. For the SI-Go contrast, preSMA ($t_{22} = 2.127$, $P = 0.045$), left vmPFC ($t_{22} = 2.746$, $P = 0.012$), and right vmPFC ($t_{22} = 2.629$, $P = 0.015$) showed significantly more activation after atDCS than the sham condition (Fig. 5b). Critically, to explore the predictive power which these three ROIs may have on each participant's behavioral performance, we calculated an index denoting the percentage of SSRT improvement ($\% \text{ of SSRT improvement} = 100\% \times (\text{SSRT}_{sham} - \text{SSRT}_{anodal}) / \text{SSRT}_{sham}$), and performed a correlation analysis with each of these separate ROIs. Results showed that enhanced vmPFC (MNI coordinate of 14, 48, -8) activity was positively correlated with SSRT decrement (improvement) across subjects ($r = 0.417$, $P = 0.048$; Fig. 5c), while the other two ROIs were not significantly correlated with such measures of behavioral improvement.

Functional connectivity of the preSMA

The PPI analyses revealed increased coupling between preSMA and vmPFC, and posterior cingulate cortex after atDCS stimulation when participants successfully withheld their responses (SI). In addition, the vmPFC in the PPI result overlies with the vmPFC in the GLM (stop - rest) contrast (Fig. 6). Although such task-related change in functional connectivity between preSMA and vmPFC provides an explanation for the atDCS-induced increase in vmPFC

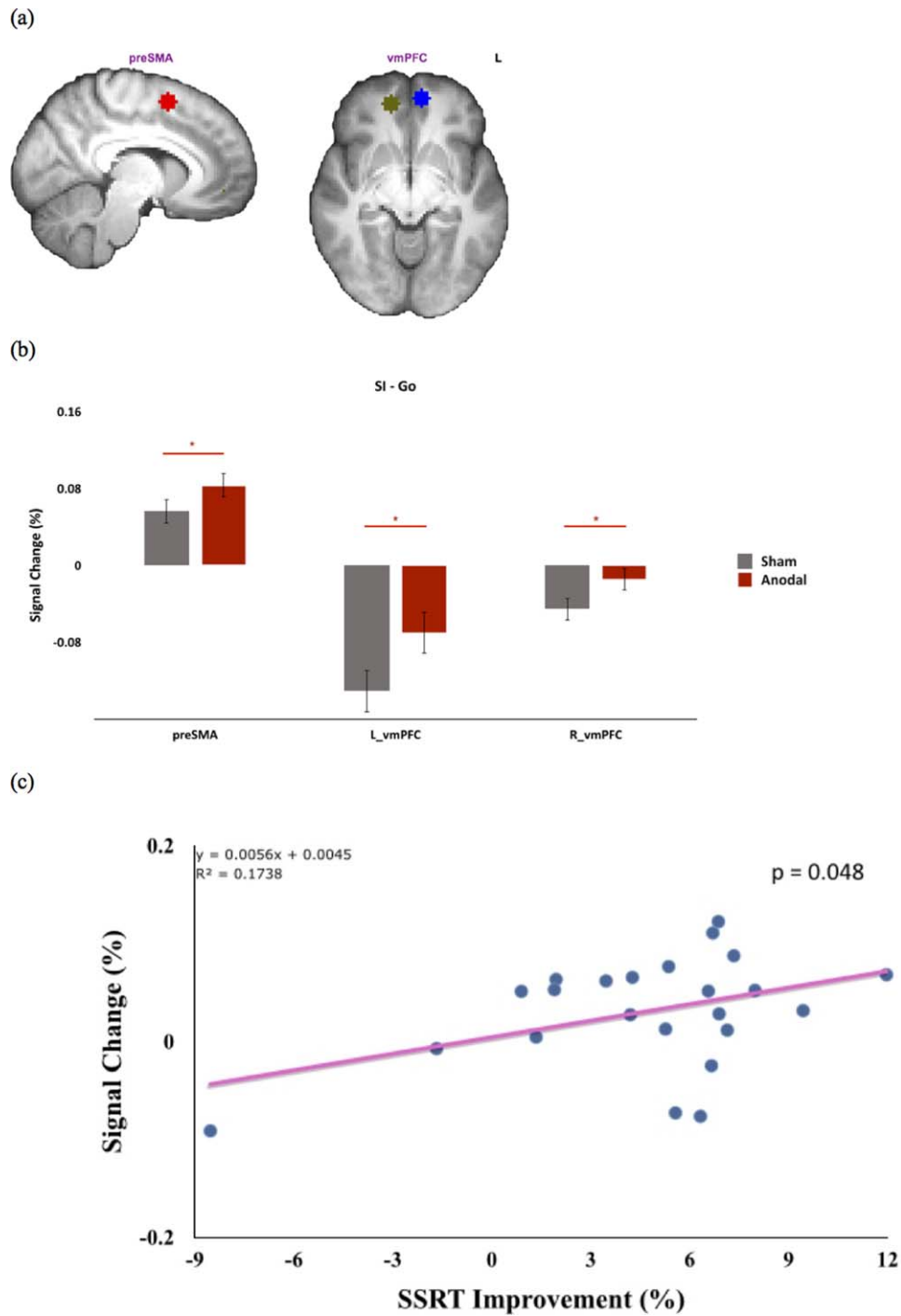


Figure 5.

Increased frontal activation during response inhibition by atDCS. (a) Three ROI masks, preSMA and bilateral vmPFC, were defined based on the results from the Stop contrasts. (b) ROI results showed increased activations in right preSMA and vmPFC after atDCS, as opposed to sham atDCS. (c) A positive correlation

was observed between individual right-vmPFC activations and their SSRT facilitation [% of SSRT improvement = $100\% \times (\text{SSRT}_{\text{sham}} - \text{SSRT}_{\text{anodal}}) / \text{SSRT}_{\text{sham}}$] (*: $P < 0.05$). [Color figure can be viewed in the online issue, which is available at wileyonlinelibrary.com.]

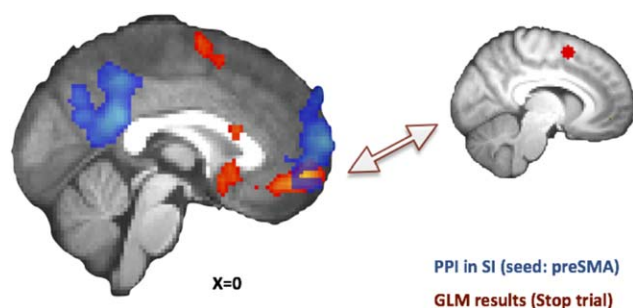


Figure 6.

PPI results from the atDCS condition showed an increase in functional connectivity between preSMA and vmPFC in the SI condition, which overlaps with the vmPFC from the stop > rest contrast from the GLM. [Color figure can be viewed in the online issue, which is available at wileyonlinelibrary.com.]

BOLD activity, both the direction and magnitude of the coupling is not known. We also performed ROI analysis to estimate PPI between preSMA and vmPFC in both SI and SR conditions. We found an increase in functional connectivity after atDCS only in the SI trials ($t_{22} = 2.588$, $P = 0.017$) and not in the SR trials ($t_{22} = 0.3$, $P = 0.767$). However, there was no correlation between changes in the preSMA-vmPFC functional connectivity and SSRT improvement ($r = -0.12$, $P = 0.589$), which implied that individual behavioral performance was not associated with the change of preSMA-vmPFC connectivity.

DISCUSSION

The role of the preSMA in response inhibition was investigated by a combination of fMRI and tDCS techniques. Consistent with previous fMRI studies, preSMA, rIFG, bilateral DLPFC and PPC showed higher activations when individuals performed efficient stopping (SI) compared with correct action execution (Go). Anodal tDCS over preSMA improved participants' inhibitory control and accelerated the stopping process (decreased SSRTs), while leaving other behavioral indexes such as Go RT and SR RT unchanged. Hence, increased activation in the preSMA was observed after atDCS as opposed to the sham condition when stopping processes occurred. In addition, vmPFC—a region not commonly implicated in response inhibition—was identified to have higher BOLD response in efficient stopping after atDCS stimulation. It is also the only region whose activation difference was predictive of the individual improvement in behavioral performance.

Although several fMRI and TMS studies have suggested a critical role for preSMA in response inhibition and selection via the use of correlational methods and temporary impairment [Neubert et al., 2010, 2011; Rushworth et al., 2002; Sharp et al., 2010; Taylor et al., 2007; Zandbelt et al., 2013], only few studies have demonstrated a behavioral improvement via the use of tDCS over preSMA [Hsu

et al., 2011; Liang et al., 2014; Reinhart and Woodman, 2014]. In this study, a higher BOLD response in the preSMA after atDCS supports our hypotheses, as well as previous findings from other laboratories, that higher preSMA activation is associated with faster stopping speed. This result is also consistent with the assumption in the literature that atDCS should modulate the activation level of the site of stimulation; thus, the simple-modulation idea that is often assumed in the field of brain stimulation is to some extent verified here.

What is more intriguing here is perhaps the observation of atDCS-induced higher vmPFC activations in stop trials. The vmPFC, although highly implicated in several important cognitive functions such as value-based decision-making, risk, and uncertainty [Figner et al., 2010; Hare et al., 2009; Kable and Glimcher, 2010; Xue et al., 2012], has rarely been reported in response inhibition literatures. To our knowledge, the only study in the field that also observed vmPFC activation in the context of inhibitory control was conducted by Li et al. [2010] in a group of cocaine-dependent patients. These authors gave cocaine-dependent participants methylphenidate, a neural stimulant that is applied intravenously, and they observed an SSRT improvement that was associated with vmPFC activation. Beyond validating our observed activation here in vmPFC, this also makes for quite an interesting comparison with our current results. Although the methods of induced neural stimulation (stimulant drug vs. electrical stimulation) and participants (substance abusers vs. health volunteers) were different, both methylphenidate and atDCS induced a short-term and within-subject activation change in vmPFC. This similar pattern seems to indicate that perhaps stimulants and electrical stimulation may share certain similarities in terms of neural substrates or chemistry, which may help explain the effect of preSMA-tDCS that induced activation in vmPFC. In this light, it is known that stimulants can modulate frontal cortex activity by altering local high gamma oscillations [e.g., Berke, 2009] or dopaminergic pathways [Kuo et al., 2008; Wagner et al., 2007]. It is possible that similar mechanisms are at work here behind the atDCS effect as well, though much work needs to be done to substantiate this speculation.

Another important uniqueness that sets the current study and the Li et al. [2010] study apart from the literature on response inhibition is the fact that both studies are the only ones in the field that have employed a within-subject design and with a short-term artificially induced boost in performance. Other studies to date have compared high- and low-performers in a between-subject design, mostly because behavioral improvement in inhibitory control is difficult to induce within individuals. Consequently, our current understanding of the stopping network is solely based on between-subject neuroimaging data, with no information on the neural mechanisms behind within-individual improvements. From this perspective, there are two similarities between our and Li

et al. studies. First, tDCS and stimulant drug are short-term boost in behavioral performance that does not last long; second, these two methods induced within-individual improvements. Whether the additional recruitment of vmPFC is a result of the former or latter, or both, requires further research in the future. For now, at least one study by Berkman et al. [2014] provides support for the latter explanation. These authors gave participants 10 training sessions across a span of 3 weeks and observed improvement in SSRT. Importantly, they found activations from the same areas within the original inhibitory network, though differing in magnitude. In other words, long-term behavioral training seems to elevate response inhibition by recruiting the original stopping network, whereas temporary stimulation via methylphenidate or atDCS recruits additional areas such as the vmPFC to aid the stopping network.

Although not a part of the inhibitory control network, we note that the function of the vmPFC must be directly related to, yet independent from, the overall response inhibition processes. The direct relationship to the stopping processes is likely because vmPFC BOLD response was highly predictive of the atDCS-induced behavioral improvement. However, such functional facilitation should be independent from the general stopping processes since previous fMRI studies using similar paradigms have not observed signals from vmPFC in a stopping related contrast (i.e., SI-Go or SI-SR). One recent fMRI study using a probabilistic reasoning paradigm with noisy feedback that manipulated the combinations of stimuli and response (rule switching) to probe the neural correlates of action switching has suggested vmPFC activation to be associated with the extent to which a strategy is applicable to the current situation [Donoso et al., 2014]. That is, vmPFC makes probabilistic inferences between current external contingencies and ongoing behavioral strategy and evaluates whether it is time to move on and switch to new strategies. Consistent with this view, in the context of the stop signal task, participants are faced with the uncertainty of whether to release or withhold motor actions. Therefore, if one views the stopping process as a form of motor reprogramming or action re-selection [see, Neubert et al., 2011, for compelling evidence using double-pulse TMS], then probabilistic inference and program evaluation would seem to be a suitable facilitator for such processes. Thus, it is possible that preSMA acquires the information about task reliability and stop-signal probability from vmPFC to form a more efficient action set to achieve better performance in the context of the stop-signal paradigm. This would also be consistent with the criterion that vmPFC functioning is directly related to, but independent from, cognitive and inhibitory control [Shenhav et al., 2013]. This enhanced functional connectivity between the vmPFC and preSMA

In the tDCS literature, it is not uncommon to observe activation in areas other than the stimulation site [e.g., Ellison et al., 2014]. One plausible explanation for the current

results is that offline atDCS may have facilitated neural activity within the preSMA and further transformed this facilitation effect via functional connectivity to the vmPFC. The reverse direction of effect would be less plausible for two reasons: (1) the stimulation effect must have first entered the cortex via preSMA and further propagated beyond that point and (2) results from our effective connectivity analysis revealed that atDCS facilitated the correlation of neural activity between preSMA and vmPFC when participants performed correct stops, a cognitive function that preSMA is known to mediate. As of now, although the precise mechanisms behind the facilitating effect of atDCS remain largely unclear, there are some recent studies documenting that electrical stimulation also seems to have a positive effect on dopaminergic activity [Nitsche et al., 2006] and neural oscillations [Jacobson et al., 2012]. Importantly, one notable recent study analyzed the neural oscillation signals in terms of their signal complexity, or entropy, over different time scales while participants performed the stop-signal task, with or without electrical stimulation [Liang et al., 2014]. Authors found that atDCS over preSMA also effectively increased the complexity of the signals originating from the frontal lobe, which was coupled with improved SSRT performance. Additionally, evidence from resting state fMRI studies showed that preSMA is functionally connected with PFC, parietal lobe, thalamus, and basal ganglia [Zhang et al., 2012]. Since preSMA is functionally connected to the vmPFC, observations of changing frontal activity, either here or those reported by Liang et al. [2014], are quite plausible. Thus, although vmPFC has not been widely implicated in the inhibitory control network, its functions may nevertheless be quite relevant to the processes by which successful inhibitory control occurs. If this is true, it becomes intriguing why such functionally relevant region was never implicated in any stop-signal studies in healthy individuals. One possible explanation is that perhaps vmPFC is positioned on or near the path of least electrical resistance, thus benefitting from overflowing currents in this study. More imaging and modeling studies are needed to precisely map out the directions of current flow in the brain.

Regarding individual differences and the generalizability of tDCS, it is worth noting that there were two individuals whose performance did not improve after atDCS in this study (Fig. 5c). This lack of tDCS effect is possibly due to homeostatic plasticity [Lang et al., 2004; Siebner et al., 2004], where individuals' pre-existing excitability state can alter their stimulation outcomes, as evidenced by the TMS literature [Silvanto et al., 2008]. This can be one possible explanation for the two individuals whose performance did not improve.

CONCLUSIONS

In this study, we combined tDCS and fMRI to trace the neural underpinnings of the facilitatory effect of tDCS.

Beyond observing activation in the usual inhibitory network comprised of preSMA, rIFG, bilateral DLPFC, and bilateral PPC, the novel finding here comes from the robust activation in vmPFC, an area that has never been implicated in the literature of cognitive control in healthy participants. In addition, vmPFC activation level was predictive of each individual's improvement in cognitive control, suggesting that vmPFC was indeed related to inhibition performance instead of a mere byproduct of brain stimulation. This is the first study that demonstrates (1) vmPFC may be better-suited to explain individual-specific improvement in cognitive control than the usual inhibitory network; (2) the neural mechanisms behind the short and rapid behavioral improvement brought forth by brain stimulation may be quite different from, yet functionally connected to, the region/network responsible for normal and long-term cognitive training. (3) preSMA activation has been found useful in segregating low from high performers in cognitive control (between-subject), vmPFC may be better-suited to explain individual-specific improvement in inhibitory control (within-subject).

ACKNOWLEDGMENT

The authors are grateful to Neil Muggleton's insightful comment and suggestion.

REFERENCES

- Antal A, Keeser D, Priori A, Padberg F, Nitsche MA (2015): Conceptual and procedural shortcomings of the systematic review "Evidence that transcranial direct current stimulation (tDCS) generates little-to-no reliable neurophysiologic effect beyond MEP amplitude modulation in healthy human subjects: A systematic review "by Horvath and co-workers. *Brain Stimul* 8: 846–849.
- Aron AR, Poldrack RA (2006): Cortical and subcortical contributions to Stop signal response inhibition: Role of the subthalamic nucleus. *J Neurosci* 26:2424–2433.
- Band GP, van der Molen MW, Logan GD (2003): Horse-race model simulations of the stop-signal procedure. *Acta Psychol (Amst)* 112:105–142.
- Beckmann CF, Smith SM (2004): Probabilistic independent component analysis for functional magnetic resonance imaging. *IEEE Trans Med Imaging* 23:137–152.
- Berke JD (2009): Fast oscillations in cortical-striatal networks switch frequency following rewarding events and stimulant drugs. *Eur J Neurosci* 30:848–859.
- Berkman ET, Kahn LE, Merchant JS (2014): Training-induced changes in inhibitory control network activity. *J Neurosci* 34: 149–157.
- Cisler JM, Bush K, Steele JS (2014): A comparison of statistical methods for detecting context-modulated functional connectivity in fMRI. *Neuroimage* 84:1042–1052.
- Chen CY, Muggleton NG, Tzeng OJ, Hung DL, Juan CH (2009): Control of prepotent responses by the superior medial frontal cortex. *Neuroimage* 44:537–545.
- Cohen JR, Poldrack RA (2008): Automaticity in motor sequence learning does not impair response inhibition. *Psychon Bull Rev* 15:108–115.
- Diamond A (2013): Executive functions. *Annu Rev Psychol* 64: 135–168.
- Donoso M, Collins AG, Koechlin E (2014): Human cognition. *Foundations of human reasoning in the prefrontal cortex. Science* 344:1481–1486.
- Duann JR, Ide JS, Luo X, Li CS (2009): Functional connectivity delineates distinct roles of the inferior frontal cortex and pre-supplementary motor area in stop signal inhibition. *J Neurosci* 29:10171–10179.
- Ellison A, Ball KL, Moseley P, Dowsett J, Smith DT, Weis S, Lane AR (2014): Functional interaction between right parietal and bilateral frontal cortices during visual search tasks revealed using functional magnetic imaging and transcranial direct current stimulation. *PLoS One* 9:e93767.
- Esterman M, Tamber-Rosenau BJ, Chiu YC, Yantis S (2010): Avoiding non-independence in fMRI data analysis: Leave one subject out. *Neuroimage* 50:572–576.
- Figner B, Knoch D, Johnson EJ, Krosch AR, Lisanby SH, Fehr E, Weber EU (2010): Lateral prefrontal cortex and self-control in intertemporal choice. *Nat Neurosci*, 13:538–539.
- Friston KJ, Buechel C, Fink GR, Morris J, Rolls E, Dolan RJ (1997): Psychophysiological and modulatory interactions in neuroimaging. *Neuroimage* 6:218–229.
- Hare TA, Camerer CF, Rangel A (2009): Self-control in decision-making involves modulation of the vmPFC valuation system. *Science* 324:646–648.
- Horvath JC, Forte JD, Carter O (2015a): Evidence that transcranial direct current stimulation (tDCS) generates little-to-no reliable neurophysiologic effect beyond MEP amplitude modulation in healthy human subjects: a systematic review. *Neuropsychologia* 66:213–236.
- Horvath JC, Forte JD, Carter O (2015b): Quantitative review finds no evidence of cognitive effects in healthy populations from single-session transcranial direct current stimulation (tDCS). *Brain Stimul* 8:535–550.
- Hsu TY, Tseng LY, Yu JX, Kuo WJ, Hung DL, Tzeng OJ, Walsh V, Muggleton N, Juan CH (2011): Modulating inhibitory control with direct current stimulation of the superior medial frontal cortex. *Neuroimage* 56:2249–2257.
- Jacobson L, Ezra A, Berger U, Lavidor M (2012): Modulating oscillatory brain activity correlates of behavioral inhibition using transcranial direct current stimulation. *Clin Neurophysiol* 123: 979–984.
- Jacobson L, Javitt DC, Lavidor M (2011): Activation of inhibition: Diminishing impulsive behavior by direct current stimulation over the inferior frontal gyrus. *J Cogn Neurosci* 23: 3380–3387.
- Jenkinson M, Bannister P, Brady M, Smith S (2002): Improved optimization for the robust and accurate linear registration and motion correction of brain images. *Neuroimage* 17:825–841.
- Juan CH, Muggleton NG (2012): Brain stimulation and inhibitory control. *Brain Stimul* 5:63–69.
- Kable JW, Glimcher PW (2010): An "as soon as possible" effect in human intertemporal decision making: Behavioral evidence and neural mechanisms. *J Neurophysiol* 103:2513–2531.
- Kuo MF, Paulus W, Nitsche MA (2008): Boosting focally-induced brain plasticity by dopamine. *Cereb Cortex* 18:648–651.
- Lang N, Siebner HR, Ernst D, Nitsche MA, Paulus W, Lemon RN, Rothwell JC (2004): Preconditioning with transcranial direct

- current stimulation sensitizes the motor cortex to rapid-rate transcranial magnetic stimulation and controls the direction of after-effects. *Biol Psychiatry* 56:634–639.
- Li CS, Huang C, Constable RT, Sinha R (2006): Imaging response inhibition in a stop-signal task: Neural correlates independent of signal monitoring and post-response processing. *J Neurosci* 26:186–192.
- Li CS, Morgan PT, Matuskey D, Abdelghany O, Luo X, Chang JL, et al. (2010): Biological markers of the effects of intravenous methylphenidate on improving inhibitory control in cocaine-dependent patients. *Proc Natl Acad Sci USA* 107:14455–14459.
- Li LM, Uehara K, Hanakawa T (2015): The contribution of interindividual factors to variability of response in transcranial direct current stimulation studies. *Front Cell Neurosci* 9:181.
- Liang WK, Lo MT, Yang AC, Peng CK, Cheng SK, Tseng P, Juan CH (2014): Revealing the brain's adaptability and the transcranial direct current stimulation facilitating effect in inhibitory control by multiscale entropy. *Neuroimage* 90:218–234.
- Logan GD, Cowan WB, Davis KA (1984): On the ability to inhibit simple and choice reaction time responses: a model and a method. *J Exp Psychol Hum Percept Perform* 10:276–291.
- Moffitt TE, Arseneault L, Belsky D, Dickson N, Hancox RJ, Harrington H, et al. (2011): A gradient of childhood self-control predicts health, wealth, and public safety. *Proc Natl Acad Sci USA* 108:2693–2698.
- Neubert FX, Mars RB, Buch ER, Olivier E, Rushworth MF (2010): Cortical and subcortical interactions during action reprogramming and their related white matter pathways. *Proc Natl Acad Sci USA* 107:13240–13245.
- Neubert FX, Mars RB, Olivier E, Rushworth MF (2011): Modulation of short intra-cortical inhibition during action reprogramming. *Exp Brain Res* 211:265–276.
- Nitsche MA, Lampe C, Antal A, Liebetanz D, Lang N, Tergau F, Paulus W (2006): Dopaminergic modulation of long-lasting direct current-induced cortical excitability changes in the human motor cortex. *Eur J Neurosci* 23:1651–1657.
- Nitsche MA, Doemkes S, Karakose T, Antal A, Liebetanz D, Lang N, et al. (2007): Shaping the effects of transcranial direct current stimulation of the human motor cortex. *J Neurophysiol* 97:3109–3117.
- Reinhart RM, Woodman GF (2014): Causal control of medial-frontal cortex governs electrophysiological and behavioral indices of performance monitoring and learning. *J Neurosci* 34:4214–4227.
- Rushworth MF, Hadland KA, Paus T, Sipila PK (2002): Role of the human medial frontal cortex in task switching: A combined fMRI and TMS study. *J Neurophysiol* 87:2577–2592.
- Sharp DJ, Bonnelle V, De Boissezon X, Beckmann CF, James SG, Patel MC, Mehta MA (2010): Distinct frontal systems for response inhibition, attentional capture, and error processing. *Proc Natl Acad Sci USA* 107:6106–6111.
- Shenhav A, Botvinick MM, Cohen JD (2013): The expected value of control: An integrative theory of anterior cingulate cortex function. *Neuron* 79:217–240.
- Siebner HR, Lang N, Rizzo V, Nitsche MA, Paulus W, Lemon RN, Rothwell JC (2004): Preconditioning of low-frequency repetitive transcranial magnetic stimulation with transcranial direct current stimulation: Evidence for homeostatic plasticity in the human motor cortex. *J Neurosci* 24:3379–3385.
- Silvanto J, Muggleton N, Walsh V (2008): State-dependency in brain stimulation studies of perception and cognition. *Trends Cogn Sci* 12:447–454.
- Taylor PC, Nobre AC, Rushworth MF (2007): Subsecond changes in top down control exerted by human medial frontal cortex during conflict and action selection: A combined transcranial magnetic stimulation electroencephalography study. *J Neurosci* 27:11343–11353.
- Tseng P, Hsu TY, Chang CF, Tzeng OJ, Hung DL, Muggleton NG, et al. (2012): Unleashing potential: Transcranial direct current stimulation over the right posterior parietal cortex improves change detection in low-performing individuals. *J Neurosci* 32:10554–10561.
- Wagner T, Fregni F, Fecteau S, Grodzinsky A, Zahn M, Pascual-Leone A (2007): Transcranial direct current stimulation: A computer-based human model study. *Neuroimage* 35:1113–1124.
- Woolrich M (2008): Robust group analysis using outlier inference. *Neuroimage* 41:286–301.
- Wu YJ, Tseng P, Chang CF, Pai MC, Hsu KS, Lin CC, Juan CH (2014): Modulating the interference effect on spatial working memory by applying transcranial direct current stimulation over the right dorsolateral prefrontal cortex. *Brain Cogn* 91:87–94.
- Xue G, Juan CH, Chang CF, Lu ZL, Dong Q (2012): Lateral prefrontal cortex contributes to maladaptive decisions. *Proc Natl Acad Sci USA* 109:4401–4406.
- Zandbelt BB, Bloemendaal M, Hoogendam JM, Kahn RS, Vink M (2013): Transcranial magnetic stimulation and functional MRI reveal cortical and subcortical interactions during stop-signal response inhibition. *J Cogn Neurosci* 25:157–174.
- Zhang S, Ide JS, Li CS (2012): Resting-state functional connectivity of the medial superior frontal cortex. *Cereb Cortex* 22:99–111.